ELSEVIER

Journal of Hydrology 261 (2002) 74–85

Journal of Hydrology

www.elsevier.com/locate/jhydrol

Modeling of solute transport in a single fracture using streamline simulation and experimental validation

Minchul Jang*, Jaehyoung Lee[1], Jonggeun Choe[2], Joe M. Kang[3]

School of Civil, Urban and Geosystems Engineering, Seoul National University, Seoul 151-742, South Korea

Received 20 April 2001; revised 13 November 2001; accepted 19 December 2001

Abstract

Streamline simulations have been extensively used in petroleum engineering due to its computational speed and the freedom from numerical dispersion. This study applies streamline simulation to the modeling of solute transport in a single fracture and verifies the streamline method with experimental data. In order to model dispersive transport, a new term, the advection–dispersion ratio is employed, which is defined as the relative extent of advection to dispersion along streamlines. It is observed that the tracer breakthrough curves from the simulation match well with those from the experiments. In addition, the tracer displacement profiles from the simulation also show resemblance to those from the experiments. Simulations with various link transmissivity types result in no serious disparities. The distributions of time of flight and tracer breakthrough curves from the simulations using different link transmissivity types are much alike. Transport simulation is performed by allocating different advection–dispersion ratios along streamlines. Afterwards, the results are compared with the simulation result using single representative advection–dispersion ratio over the flow domain. Although streamlines actually have different advection–dispersion ratios, its effect is found to be not severe. Therefore, a representative advection–dispersion ratio can be used for modeling transport through the whole streamlines in a single fracture.

Keywords: Streamline simulation; Transport modeling; Advection–dispersion ratio; Fracture

1. Introduction

With regard to underground storages of oil, gas and nuclear deposits, it is important to effectively describe solute transport in underground environment. As storage facilities are usually located in tight rocks, the transport of leakages will occur mainly through fractures. The controlling mechanisms of solute transport in a fracture are advection, dispersion, and other processes such as sorption, biodegradation, and radioactive decay (Bear et al., 1993; Keller et al., 1999; Kitanidis, 1994). Particle tracking technique has been widely used to model advection-dominated transport. For dispersive transport, the finite difference method and the finite element method are widely used, while the random walk method can be introduced to add effects of dispersion to advection. Although the particle tracking technique is straightforward and popular in modeling advection-dominated transport, it has some drawbacks. The accuracy of this method is very sensitive to the number of particles used for tracking (Crane and Blunt, 1999). If variability in aperture becomes considerably high, a huge number

* Corresponding author. Fax: +82-2-871-8938.

E-mail addresses: jmc@geofluid.snu.ac.kr (M. Jang), jhl@geofluid.snu.ac.kr (J. Lee), jchoe@geofluid.snu.ac.kr (J. Choe), jmk@geofluid.snu.ac.kr (J.M. Kang).

[1] Fax: +82-2-871-8938.

[2] Fax: +82-2-871-8938.

[3] Fax: +82-2-873-2717.

0022-1694/02/$ - see front matter
PII: S0022-1694(02)00015-X

of particles and considerable amount of computer memory are required.

In recent decades, streamline simulation has been widely used to predict oil recovery in reservoir simulations. The computational efficiency of streamline simulation makes it possible to simulate reservoirs of multi-million cells and to develop fine-scale models that integrate detailed three-dimensional geologic and geophysical data (Datta-Gupta and King, 1995; King and Datta-Gupta, 1998). Another advantage of the streamline simulation is that the stability constraint of the underlying grid can be effectively relieved from solving one-dimensional equations along streamlines (Batycky et al., 1997, 1996; Blunt et al., 1996; Thiele et al., 1996). Batycky et al. (1997) developed a three-dimensional and multi-phase reservoir simulator in 1997. The model eliminated the numerical dispersion error and was 10–1000 times faster than existing conventional reservoir simulators.

Crane and Blunt (1999) applied the streamline simulation technique to model solute transport in porous media. Excluding the effect of dispersion, they focused on advection mechanisms and showed the effectiveness and fast calculation of streamline simulation. They made up simple synthetic cases of heterogeneous confined aquifers and compared the simulated results from their models with those from particle tracking codes and from a conventional finite difference simulator. They presented comparisons of concentration maps between the streamline method and other existing methods, which showed a good agreement.

Streamline simulation technique has been validated in several ways. Some examples are comparing simulation results with those from conventional reservoir simulators and applying streamline simulation to field reservoirs and observing production history. However, most of the streamline simulation models have not included the dispersion term in modeling transport and those validations were constrained to reservoir scale. Comparison of a model to real transport in cell-to-cell scale has not been tried sufficiently.

In this study, the streamline method was applied to model solute transport in a single fracture and the validity of the applied method was tested with experimental data. The effect of dispersion as well as advection was included in the solute transport model by employing a new term advection–dispersion ratio. The tracer breakthrough curves from the simulation and experiment were compared. The profiles of the advancement of solute from the simulations were also analyzed and whether the advancement of solute follows real trends of solute transport was investigated in experiments.

2. Streamline simulation

The main idea of streamline simulation is to decouple a multi-dimensional problem of fluid motion into multiple one-dimensional problems solved along streamlines. Fluids move along the natural streamlines rather than between discrete gridblocks as in conventional methods.

Like other conventional transport models, flow calculation is also preceded in streamline simulation. Then, flow domain is decomposed into a number of streamlines and solute transport in each streamline is interpreted as one-dimensional problem. Solving the one-dimensional transport problems analytically, we get the solutions along streamlines. Finally, the solutions are remapped onto the original flow domain and the final concentration distribution is acquired as a function of location and time. This approach makes the streamline simulation eliminate numerical dispersion errors that occur in conventional finite difference methods, enhancing computational efficiency (Batycky et al., 1997; Thiele et al., 1996).

2.1. Flow simulation

A typical approach for modeling flow within a fracture plane is to characterize the fracture as a set of parallel plate pairs with each gridblock having a uniquely defined aperture (Bear et al., 1993). The fluid flow through a variable aperture fracture was computed for the boundary condition of constant flow rate. No flow boundary conditions were applied to the sides of the fracture parallel to flow direction. The flow rate between a gridblock at (i, j) and an adjacent gridblock at $(i + 1, j)$ is calculated by cubic law

$$Q_x = \frac{b_{i+1/2j}^3 W}{12\mu} \frac{\mathrm{d}p}{\mathrm{d}x}, \tag{1}$$

where p is the pressure, b the aperture size related to link transmissivity, μ the viscosity and W is the fracture width. If steady state flow condition is assumed, summation of inflow and outflow at an arbitrary gridblok (i, j) is equivalent to zero from the law of mass conservation (Masciopinto, 1999):

$$\left(\sum Q\right)_{ij} = 0. \tag{2}$$

Then, the pressure distribution in the fracture is obtained by solving Eqs. (1) and (2) at every gridblock.

In calculating link transmissivity, four representative methods were introduced (Nicholl et al., 1999). The first one is the harmonic mean, which is frequently used for the calculation of link transmissivity:

$$b^3_{i+1/2j} = \frac{2b^3_{ij}b^3_{i+1j}}{b^3_{ij} + b^3_{i+1j}}. \tag{3}$$

The second one is the midpoints. It assumes that the arithmetic mean of the apertures in adjacent gridblocks provides a representative aperture for computing the link transmissivity as follows:

$$b^3_{i+1/2j} = \left(\frac{b_{ij} + b_{i+1j}}{2}\right)^3. \tag{4}$$

For two-dimensional flow in a porous medium with log-normally distributed transmissivity, stochastic theories predict that effective transmissivity will be given by the geometric average as follows:

$$b^3_{i+1/2j} = \sqrt{b^3_{ij}b^3_{i+1j}}. \tag{5}$$

The fourth one is the symmetric wedge, which was implemented in the study. In this approach, fracture geometry between adjacent grid blocks is approximated as a wedge, which provides a better approximation of the actual geometry

$$b^3_{i+1/2j} = \frac{2b^2_{ij}b^2_{i+1j}}{b_{ij} + b_{i+1j}} \frac{3(1 - \theta\cot\theta)}{4\tan^2(\theta/2)}, \tag{6}$$

where θ is the wedge angle between b_{ij} and b_{i+1j} (Nicholl et al., 1999).

2.2. Particle tracing along streamlines

Once the pressure field has been determined, the velocity vector field is computed to trace streamline path. If it is assumed that the velocity field varies linearly in x- or y-direction within a gridblock and is independent of the velocity in the other direction, linear interpolation can be used to calculate velocity at an arbitrary position within the gridblock. Then, the time required for a particle to reach x-exit face is given by

$$\Delta t_{ex} = \int \mathrm{d}t = \int_{x_\mathrm{i}}^{x_\mathrm{e}} \frac{\mathrm{d}x}{v_x} = \frac{1}{m_x}\ln\frac{v_{x\mathrm{e}}}{v_{x\mathrm{i}}}, \tag{7}$$

where v_x is the velocity at a given point x within the gridblock, $v_{x\mathrm{e}}$ the velocity at the exit face, $v_{x\mathrm{i}}$ the velocity at the inlet face, and m_x is the velocity gradient in x-direction (Crane and Blunt, 1999; Pollock, 1988). The exit time in y-direction is calculated the same way. Therefore, the residence time in each gridblock is determined to be the smaller one between Δt_{ex} and Δt_{ey}. Tracking all the particles according to the velocity vector field, streamline trajectories within a flow domain can be obtained.

The conventional Cartesian coordinate is converted into the coordinate system along streamlines through the concept of time of flight (TOF) (Datta-Gupta and King, 1995; Thiele et al., 1996). Mathematically TOF is defined as

$$\tau(s) = \int_0^s \frac{\mathrm{d}\zeta}{v(\zeta)}, \tag{8}$$

where ζ is the coordinate along a streamline and s is the distance along the streamline.

Accordingly, the TOF of a position along a streamline is calculated as summation of residence times in gridblocks along which the streamline takes

$$\tau = \sum_{i=1}^{N_\mathrm{b}} \Delta t_{\mathrm{e}i}, \tag{9}$$

where N_b is the number of blocks which the streamline takes along.

2.3. Mapping analytic solution along a streamline

By assuming incompressible flow in a fracture and continuous sources in one-dimension, a governing equation of advection–dispersion is obtained as

$$\frac{\partial C}{\partial t} = -v\frac{\partial C}{\partial s} + D\frac{\partial^2 C}{\partial s^2}, \tag{10}$$

where C is the concentration and D is the dispersion coefficient (Bear et al., 1993; Kitanidis, 1994). Since streamline simulation is based on the concept of multiple independent transports along one-dimensional streamlines, D in Eq. (10) describes only longitudinal dispersion.

By differentiating Eq. (8), the transformation of the coordinate is expressed as follows:

$$\frac{\mathrm{d}\tau}{\mathrm{d}s} = \frac{1}{v}, \tag{11}$$

$$v\mathrm{d}\tau = \mathrm{d}s, \tag{12}$$

$$v^2\mathrm{d}\tau^2 = \mathrm{d}s^2. \tag{13}$$

Throughout the above transformation, the advection–dispersion equation is rewritten as a transformed form with a function of TOF and time:

$$\frac{\partial C}{\partial t} = -v\frac{\partial C}{\partial s} + D\frac{\partial^2 C}{\partial s^2} = -\frac{\partial C}{\partial \tau} + \frac{D}{v^2}\frac{\partial^2 C}{\partial \tau^2}. \tag{14}$$

All terms in Eq. (14) have dimension of T^{-1}. To express Eq. (14) in a dimensionless form, time and TOF are normalized by mean residence time.

$$t_D = \frac{t}{t_0}, \qquad \tau_D = \frac{\tau}{t_0}, \tag{15}$$

where t_0 is the mean residence time within whole flow domain.

Then, Eq. (14) is expressed in a dimensionless and compact form

$$\frac{\partial C}{\partial t_D} = -\frac{\partial C}{\partial \tau_D} + \frac{1}{\mathrm{Pe}_m}\frac{\partial^2 C}{\partial \tau_D^2}, \tag{16}$$

where Pe_m is the advection–dispersion ratio defined as:

$$\mathrm{Pe}_m = \frac{v^2 t_0}{D}. \tag{17}$$

While deriving the transformed advection–dispersion equation, this study introduces a new concept of Pe_m. Pe_m denotes the average extent of advection to dispersion of transport in a fracture. A well-known Peclet number characterizes the interplay of advection and dispersion within pore scale. On the other hand, the advection–dispersion ratio characterizes that in scale of whole flow domain. Pe_m is determined for fracture domain instead of computing it at gridblock scale, not to mitigate computational efficiency of streamline simulation.

Then an approximate analytic solution to Eq. (16) can be given by:

$$\frac{C(\tau_D, t_D)}{C_0} = \frac{1}{2}\mathrm{erfc}\left(\frac{\tau_D - t_D}{2\sqrt{t_D/\mathrm{Pe}_m}}\right), \tag{18}$$

where C_0 is the source concentration at the inlet (Bear et al., 1993; Thiele et al., 1996). With the solution, the concentration at a given TOF corresponding to an arbitrary location in a streamline is calculated at a given time.

2.4. Calculation of concentration in a gridblock

The average gridblock concentration is calculated as the weighted average concentration in multiple streamlines that pass through it (Crane and Blunt, 1999; Thiele et al., 1996). The weighting in this calculation is determined according to the volume flux of each streamline

$$C_\mathrm{b} = \frac{\sum_i q_i\,\Delta\tau_i C_i(\tau)}{\sum_i q_i\,\Delta\tau_i}, \tag{19}$$

where C_b is the concentration in the gridblock, $\Delta\tau_i$ is the residence time in the gridblock along ith streamline and q_i is the volume flux of ith streamline.

For a missed gridblock, a gridblock that does not contain a streamline, a streamline is simply traced backward to the nearest gridblock containing a streamline (Crane and Blunt, 1999; Thiele et al., 1996). Then, the TOF of the missed gridblock is assigned to the sum of TOF of the nearest gridblock and the time required to trace backward to it

$$\tau_\mathrm{missed} = \overline{\tau_\mathrm{b}} + \tau_\mathrm{back}, \tag{20}$$

where $\overline{\tau_\mathrm{b}}$ is the TOF of the nearest gridblock and τ_back is the time required to trace backwards to the missed gridblock.

3. Experiment of solute transport in fractures

To observe the flow and transport pattern in fractures, experimental transparent models were established in a laboratory scale. Three transparent fracture samples made of epoxy were molded from

Table 1
Fracture properties

Sample	F1	F2	F3
Length in x-direction (cm)	29.3	29.3	29.1
Length in y-direction (cm)	4.6	4.5	4.8
Fracture volume (cm^{-3})	4.4	5.0	5.5
Mean aperture (cm)	0.032	0.038	0.038
Standard deviation (cm)	0.026	0.025	0.015
Coefficient of variation	0.82	0.66	0.40

silicone rubber casting of fractured sandstone cores following the method by Gentier (Gentier et al., 1989; Lee, 2000). Detailed information on the method may be found in the work by Hakami and Barton (1990). To make epoxy replicas of a rock fracture, the upper and lower surfaces of a rock fracture are copied using silicone rubber. These silicone rubber replicas are used as a mold for the epoxy-casting.

Using an image analyzer, two images were acquired to compare overall aperture distribution with the measured aperture distribution, one with the fracture filled with water and the other with dyed water. The latter was subtracted from the former to correct the material and light source effects. Two reciprocating pumps for dyed water and pure water are connected to avoid varying concentration of the dyed water. The effluent concentrations and images of the fracture at a constant time interval were monitored with an inline spectrophotometer and an image analyzer, respectively.

4. Results

Experiments of solute transport were conducted for three single fracture samples named F1, F2 and F3. Then, we simulated these by the streamline simulation and compared the results with those from experiments. Constant flow rate condition was applied along the flow direction, from left to right boundary in the fractures, and no-flow boundary conditions were applied on the sides parallel to the flow direction.

4.1. Input data for simulation

Aperture values in the fractures were acquired through an image analyzer and digitized into approximately 280×20 gridblocks. The geometric and statistical parameters of aperture distributions in the fractures are summarized in Table 1.

Generally, as the number of streamlines increases, the accuracies of computed concentrations at

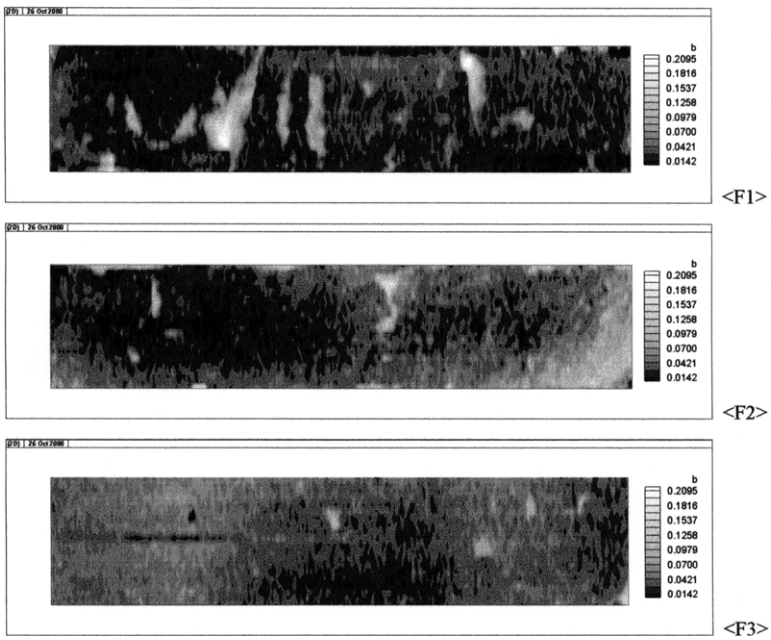

Fig. 1. Contour images of digitized aperture values in F1, F2, and F3.

Table 2
Simulation conditions

Sample	F1	F2	F3
Flow rate (cm^3/s)	0.017	0.017	0.017
Mean velocity (cm/s)	0.112	0.097	0.086
Mean residence time (s)	262	302	338
Viscosity (Pa s)	0.001	0.001	0.001
Dispersion coefficient (cm^2/s)	0.43	0.20	0.17
Advection–dispersion ratio	7.86	14.19	16.56
Dispersivity (cm)	3.78	2.06	1.87

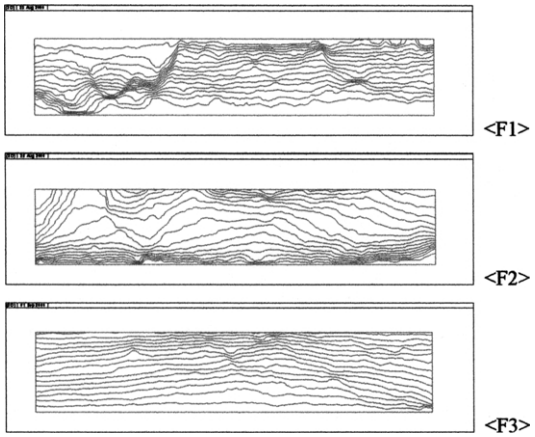

Fig. 3. Streamline distributions obtained from flow simulation.

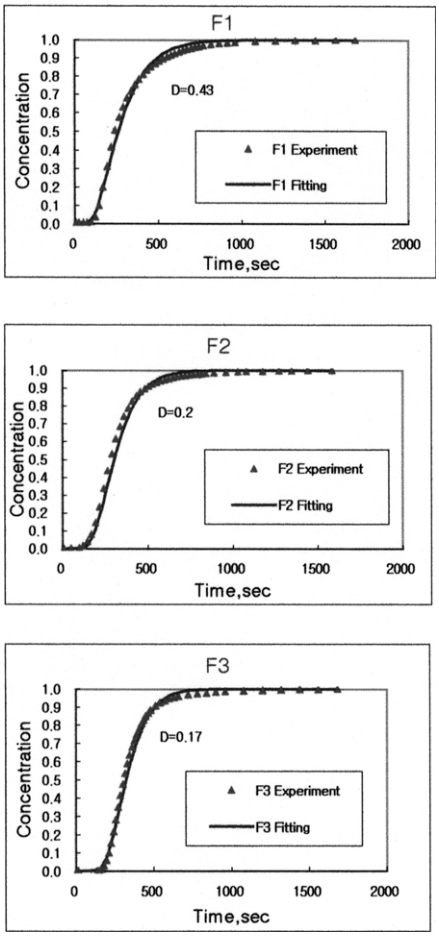

Fig. 2. Tracer breakthrough curves from experiment and the corresponding fitted curves of the analytic solution.

gridblocks are improved. However, if the number of streamlines is over a certain limit, it does not affect simulation result significantly. In this study, approximately 200 streamlines were used for each simulation.

Fig. 1 shows the aperture fields digitized for simulations. Large apertures are shown in bright colors and small apertures in dark colors. Coefficient of variation denotes how heterogeneous a field is. The fracture samples are heterogeneous in the order of F1, F2, F3 with F1 being the most heterogeneous. This trend is also observed in Fig. 1.

The input data for the simulations are summarized in Table 2. For all the cases, the flow rate was maintained at 0.017 ccm/s. The tracer breakthrough curves from experiments were fitted by the one-dimensional advection–dispersion analytic solution to determine Pe_m and representative dispersion coefficients of the fractures (Lee, 2000). Strictly speaking, it is required to investigate dispersion coefficients at all gridblocks in two-dimensional point of view. However, to make the most of efficiency of streamline simulation, the transport in fracture was conceptualized to be globally one-dimensional transport consisting of sub-streamlines and the constant dispersivity value was determined for the whole flow domain. Fig. 2 presents the tracer breakthrough curves and the fitting curves together.

4.2. Simulation results

Fig. 3 shows computed streamline fields of the fractures with the input data in Table 2. Fluid flows are

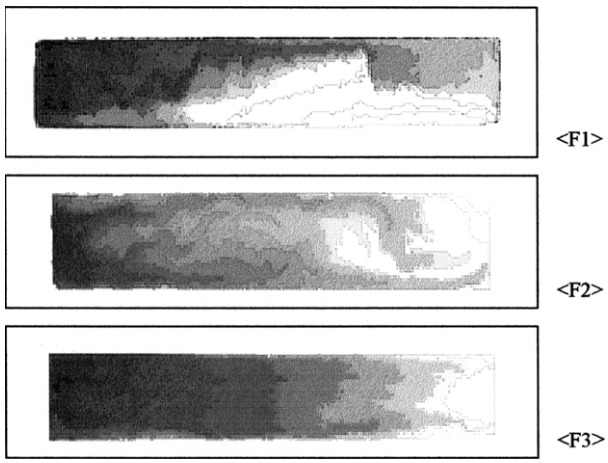

Fig. 4. Contour images of tracer displacement from the experiments.

concentrated in the area where aperture values are shown to be large in the aperture fields of Fig. 1. As expected, the streamline field of F1 appears to be the most complex among the three fractures and that of F3 represents a relatively homogeneous flow regime. After flow field was obtained, solute transport was modeled by the streamline method.

4.2.1. Comparison of simulated results with experimental data

To analyze the profiles of tracer displacements in the fractures, transport images were captured at different time levels during the experiment. The captured images were assembled and transformed into a contour image as in Fig. 4. Each contour level denotes the location of the flowing front at a specified time level. The darker contour levels represent the flowing fronts at early time and the brighter ones represent the flowing fronts at late time in the experiment.

To compare the trends of tracer displacement of the simulation and experiment, contour images of TOF distributions from the simulations are presented in Fig. 5. All the simulations were performed using the symmetric wedge for link transmissivity calculation.

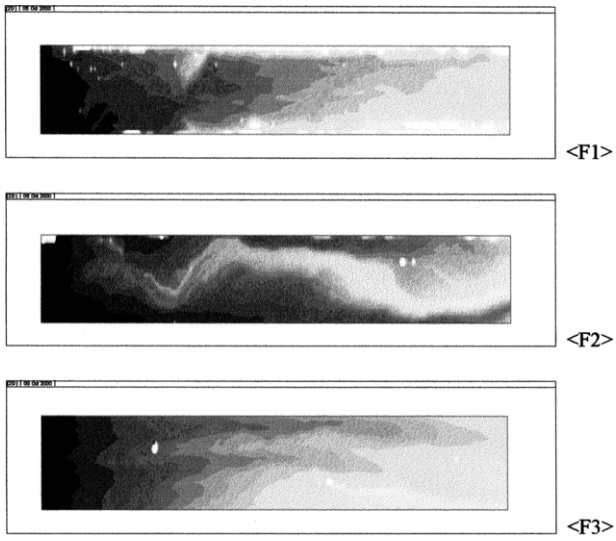

Fig. 5. TOF distributions from streamline simulations.

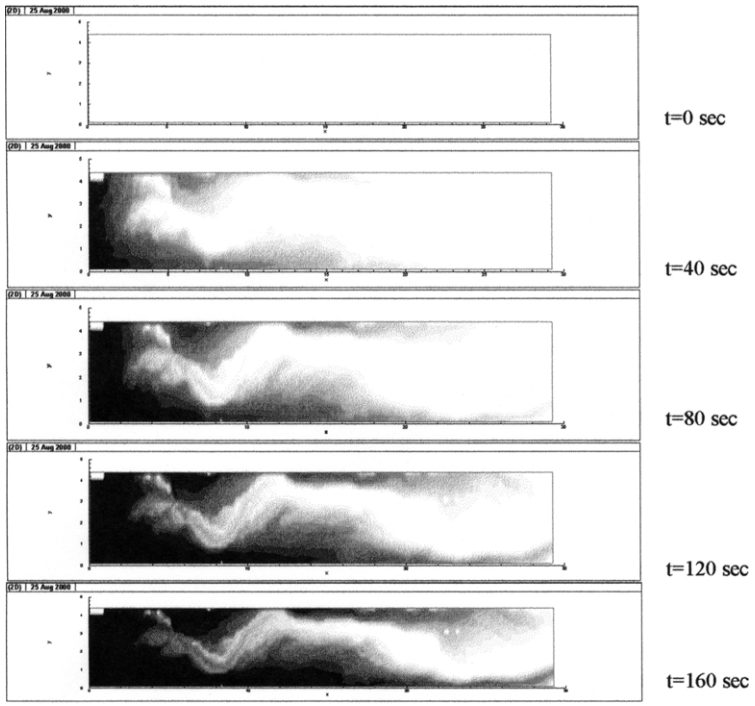

Fig. 6. Tracer displacement profiles over time from streamline simulation for F2. Each image represents tracer displacement image of F2 at 0, 40, 80, 120 and 160 s, respectively.

It is observed that the transport trends of the simulations are considerably analogous with the tracer displacement profiles from the experiment in Fig. 4.

For ⟨F3⟩, comparison of the displacement pattern between the experiment and the simulation shows a relatively poor match compared to ⟨F1⟩ and ⟨F2⟩. In Fig. 5, tracer displaces more rapidly along upper region, which may seem inconsistent to Fig. 4. However, the aperture measurements are observed to be large in the upper region in Fig. 1 and it is consistent with rapid displacement in the simulation result in Fig. 5. Therefore, the aperture field needs to be measured in a more detailed scale to improve the match between experiment and simulation results. The overall pattern, where tracers are displaced relatively straight over the whole flow domain, is observed in both Figs. 4 and 5.

To observe tracer displacement with respect to time, tracer displacement images with different time levels are presented sequentially in Fig. 6. As time increases, tracer fronts advance faster near the upper and lower boundaries of the fracture and move slowly along the paths located at the center of the fracture. An analogous trend is observed in tracer displacement profiles from experiment ⟨F2⟩ in Fig. 4.

Fig. 7 presents both the tracer breakthrough curves from experiments and those from simulations. Assuming advection-dominated transport ($Pe_m = 10\,000$) for the simulation, the tracer breakthrough curve from the simulation shows deviation from that of the experiment in ⟨F1⟩. On the other hand, when the advection–dispersion ratio acquired from the curve fitting ($Pe_m = 7.86$) in Table 2 is used, the tracer breakthrough curve from simulation matches well with that of the experiment. In ⟨F2⟩ and ⟨F3⟩, the curves with the acquired advection–dispersion ratios ($Pe_m = 14.19, 16.56$) show curvature at breakthrough time and late time, which is due to the dispersive effect. On the other hand, the curves for advection-dominated transport ($Pe_m = 10\,000$) show an abrupt concentration increase at breakthrough time and sudden stop of concentration increase at late time.

By applying the estimate of Pe_m for a fracture, streamline simulation can reflect the dispersive

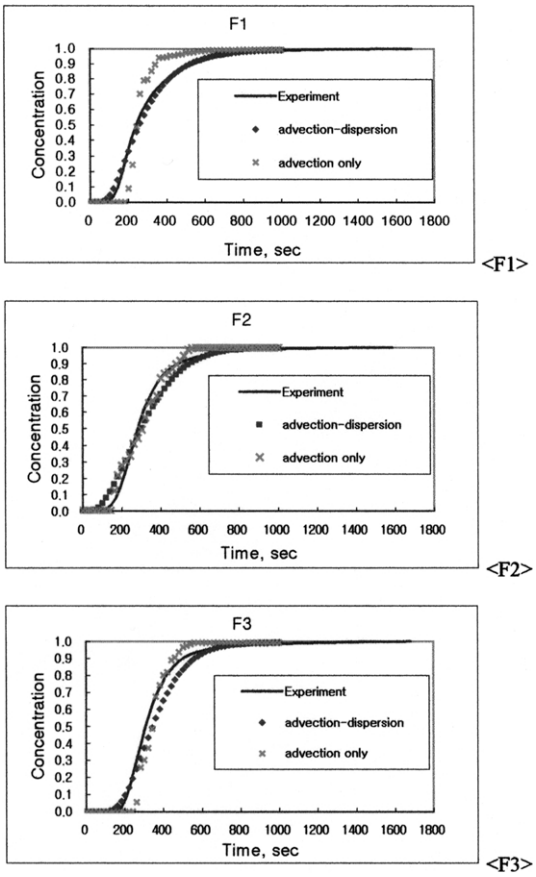

Fig. 7. Tracer breakthrough curves from streamline simulations for an advection-dominating case ($Pe_m = 1000$), the dispersion-considered case and experimental data.

transport effect and enhance the accuracy to match the tracer breakthrough curve.

Based on the compared results of the transport images and tracer breakthrough curves with experimental data, the streamline simulation can model solute transport in a fracture efficiently. It effectively models tracer displacement and reproduces tracer breakthrough curves of real transport phenomena.

4.2.2. The effects of link transmissivity types

The effects of the link transmissivity types on flow and transport simulations were analyzed with various link transmissivity formulations (Eqs. (3)–(6)). Fig. 8 shows the tracer displacement profile of F1 from the experiment and the contour images of TOF distributions from the simulations with various link transmissivity types.

By comparing the tracer displacement profile from the experiment with the TOF distributions from simulations, it is observed that the transport trends with respect to time are very analogous. Fast transport occurs in the right and upward direction both in experiment and the simulations. This therefore suggests that streamline simulation effectively models the transport profiles with respect to time. Regarding the effect of link transmissivity on the tracer displacement profiles, it is observed that the tracer displacement profiles from symmetric wedge, harmonic mean, geometric average, and midpoints do not show a significant difference. Although the distributions of TOF show local discrepancies, the global trends of the tracer displacements are much alike.

The tracer breakthrough curves from experiment and simulations with various link transmissivity types are presented together in Fig. 9. Similar to the tracer displacement profiles, the tracer breakthrough curves with various link transmissivity types marked little disparity from each other. All the curves match well with the curve from experiment. These results indicate that the link transmissivity types do not affect streamline simulation seriously when constant flow boundary conditions are applied along the flow direction.

4.2.3. Analysis on the advection–dispersion ratio

In the above simulations, single value of Pe_m was assumed for the entire flow domain. Since the average velocity of each streamline is different, the dispersion coefficient values vary along different streamlines. In the simplified form, dispersion coefficient is expressed as

$$D_x = \alpha v_x + D_{\mathrm{d}}, \tag{21}$$

where α is the dispersivity and D_{d} is the molecular diffusion coefficient.

Assuming the effect of molecular diffusion is negligible, the dispersion coefficient of the nth streamline can be approximated as follows

$$D_n \approx \alpha v_n, \tag{22}$$

where v_n is the velocity of nth streamline.

With the dispersivity value determined from the curve fitting of the tracer breakthrough curve in

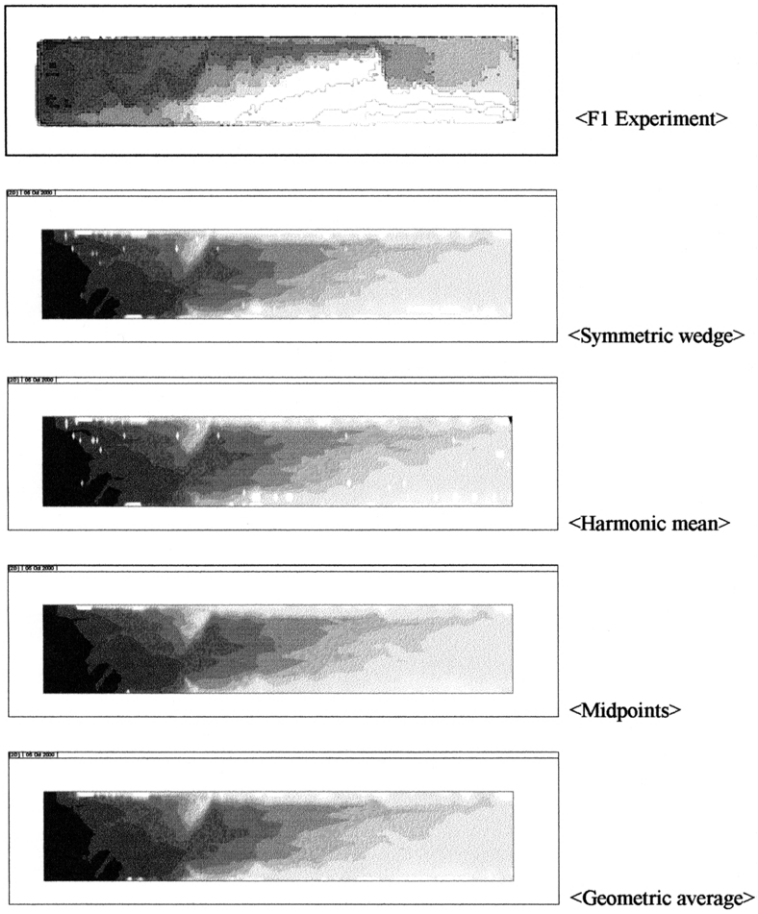

Fig. 8. TOF distributions of F1 from streamline simulations with various transmissivity types.

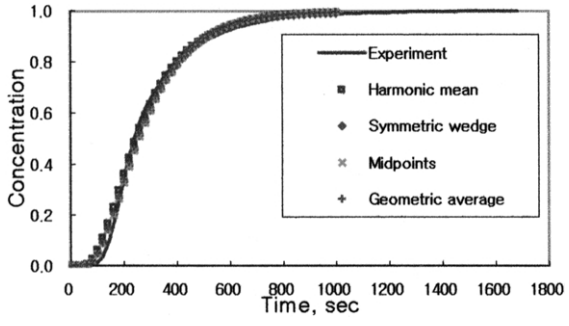

Fig. 9. Tracer breakthrough curves from streamline simulation on F1 with various transmissivity types.

Table 2 and the various values for average velocity of each streamline, the dispersion coefficient of every streamline was computed independently and used for the simulation. Fig. 10 presents the distributions of Pe_m along the streamlines and tracer breakthrough curves from the simulation with various Pe_ms along the streamlines. As known from the definition of Pe_m, when Pe_m along a streamline is high, the velocity along the streamline is relatively high compared to the dispersivity. Accordingly, advection has a higher influence on the transport along the streamline than dispersion. The histograms of Pe_m in F1 and F3 are negatively skewed, therefore many streamlines are influenced more by advection than by dispersion. In contrast, the histogram of Pe_m in F2 is positively skewed. It

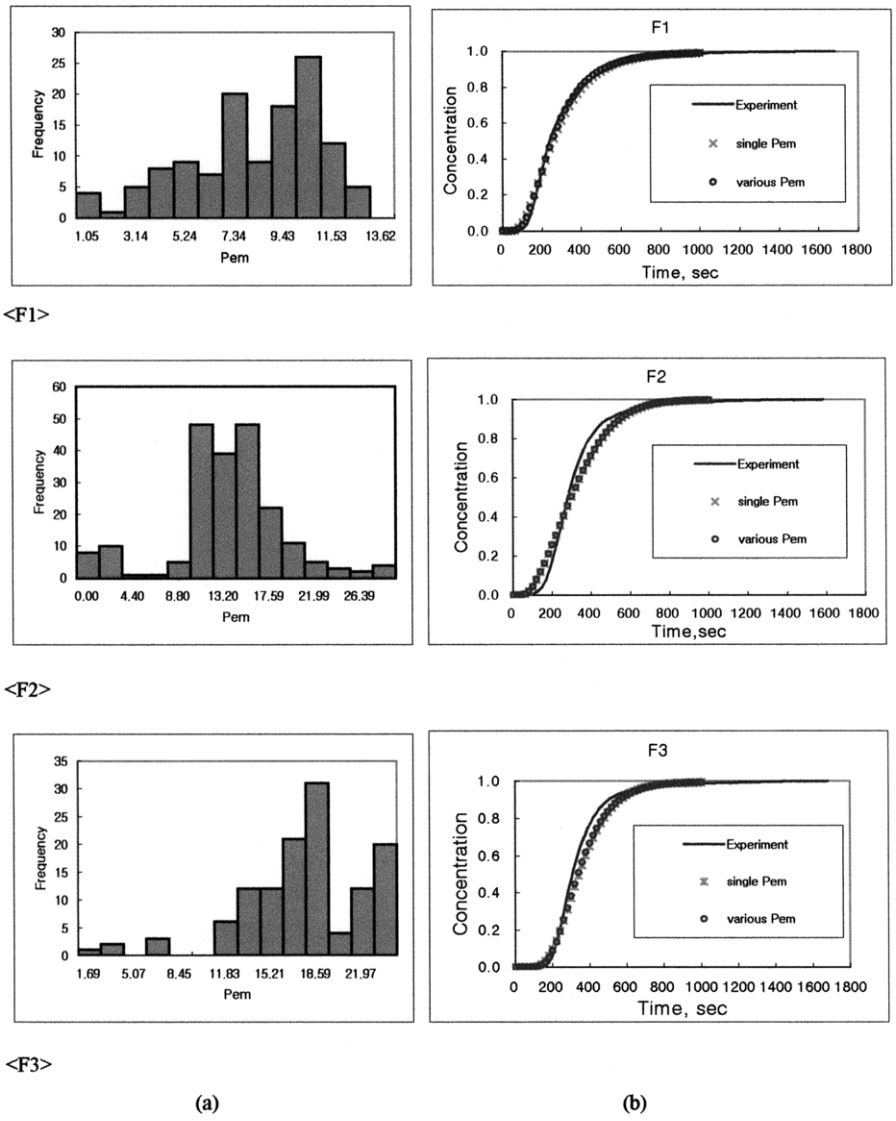

Fig. 10. (a) Distributions of Pe_m for simulation with various Pe_m. (b) Comparisons of tracer breakthrough curve from simulation with single representative Pe_m and tracer breakthrough curve from simulation with various Pe_m along streamlines.

means that many streamlines are influenced more by dispersion compared to F1 and F3.

For all the three cases, it is observed that the tracer breakthrough curves with the single representative Pe_m and various Pe_ms on streamlines do not result in severe disparity in Fig. 10b. The effect of allocating different Pe_ms along streamlines is not significant in these cases. Standard deviations of Pe_ms are 3.5, 5.8, and 4.5, respectively. These values denote relatively small deviations from representative Pe_ms thus the single representative Pe_m is enough for the streamline simulation.

In the transport experiments, major flow occurs in one direction (from left to right) and no flow boundary condition is applied perpendicular to the flow direction. It diminishes the effect of complicated transverse dispersion and resulted in good match of tracer breakthrough curves.

5. Conclusions

Streamline simulation was applied to model solute transport in a single fracture and the validity of streamline simulation was tested with experimental data. To model the effect of dispersive transport, a new term, the advection–dispersion ratio was introduced. It denotes the extent of advection relative to dispersion in a transformed equation for solute transport. The tracer breakthrough curves from the simulation excellently matched those from the solute transport experiments. In addition, the TOF distributions of streamline simulation show similarity to the images of flowing front distributions from the experiment. This indicates that streamline simulation can effectively model solute transport in a single fracture.

The effect of link transmissivity types on solute transport modeling by streamline simulation was also investigated. The results indicate that link transmissivity types do not influence much on both the tracer breakthrough curves and the tracer displacement profiles.

Allocating different Pe_ms along streamlines does not make large difference from the case of one representative Pe_m in transport simulation. Although streamlines have different Pe_m, the effect of Pe_m is not severe for streamline simulation. Therefore, a representative Pe_m can be used for modeling transport in a single fracture under the conditions that flow occurs dominantly in one direction and Pe_ms along streamlines do not deviate much from a representative Pe_m.

Since complex multi-dimensional transport is interpreted as transport along independent one-dimensional streamlines, transverse dispersion between streamlines was not described here. Integration of transverse dispersion into streamline simulation is required for future works. However, it should be investigated seriously whether the integration of transverse dispersion weakens the merit of streamline simulation or computational efficiency.

Acknowledgements

This work was conducted through the Research Institute of Engineering Science at Seoul National University, Korea.

References

Batycky, R.P., Thiele, M.R., Blunt, M.J., 1996. A streamline simulator to model field scale three-dimensional flow. Proceedings of the Fifth European Conference on Mathematics of Oil Recovery, European Association of Geoscience and Engineering.

Batycky, R.P., Blunt, M.J., Thiele, M.R., 1997. A 3D field scale streamline-based simulator. SPE Reservoir Engng 12, 246–254.

Bear, J., Tsang, C.F., de Marsily, G., 1993. Flow and Contaminant Transport in Fractured Rock. Academic Press, San Diego.

Blunt, M.J., Liu, K., Thiele, M.R., 1996. A generalized streamline method to predict reservoir flow. Petrol. Geosci. 2, 259–269.

Crane, M.J., Blunt, M.J., 1999. Streamline-based simulation of solute transport. Water Resour. Res. 35 (10), 3061–3077.

Datta-Gupta, A., King, M.J., 1995. A semianalytic approach to tracer flow modeling in heterogeneous permeable media. Adv. Water Resour. 18, 9–24.

Gentier, S., Billaux, D., Vliet, L., 1989. Laboratory testing of the voids of a fracture. Rock Mech. Rock Engng 22 (5), 149–157.

Hakami, E., Barton, N., 1990. Aperture measurement and flow experiments using transparent rock joints. In: Barton, N., Stephansson, O. (Eds.), Proceedings of the International Symposium on Rock Joints. Balkema, Rotterdam, pp. 383–390.

Keller, A.A., Roberts, P.V., Blunt, M.J., 1999. Effect of fracture aperture variations on the dispersion of contaminants. Water Resour. Res. 35 (1), 55–63.

King, M.J., Datta-Gupta, A., 1998. Streamline simulation: a current perspective. In Situ 22 (1), 91–117.

Kitanidis, P.K., 1994. Particle-tracking equations for the solution of the advection–dispersion equation with variable coefficients. Water Resour. Res. 30 (11), 3225–3227.

Lee, J.H., 2000. An experimental study for the effect of variable apertures on solute transport and two-phase flow in fractured rocks. PhD dissertation. Seoul National University, Korea, February 2000.

Masciopinto, C., 1999. Particles' transport in a single fracture under variable flow regimes. Adv. Engng Software 30, 327–337.

Nicholl, M.J., Rajaram, H., Glass, R.J., Detwiler, R., 1999. Saturated flow in a single fracture: evaluation of the Reynolds equation in measured aperture fields. Water Resour. Res. 35 (11), 3361–3373.

Pollock, D.W., 1988. Semi-analytical computation of pathlines for finite-difference models. Ground Water 26 (6), 743–750.

Thiele, M.R., Batycky, R.P., Blunt, M.J., Orr Jr., F.M., 1996. Simulating flow in heterogeneous media using streamtubes and streamlines. SPE Reservoir Engng 10, 5–12.